

IN VITRO STUDY OF COLLAGEN COATING BY ELECTRODEPOSITION ON ACRYLIC BONE CEMENT WITH ANTIMICROBIAL POTENTIAL

S. CAVALU, V. SIMON^a, F. BANICA

University of Oradea, Faculty of Medicine and Pharmacy, 410068 Oradea, Romania

^aBabes-Bolyai University, Faculty of Physics & Institute of Interdisciplinary Research in Bio-Nano-Sciences, 400084 Cluj-Napoca, Romania

New acrylic bone cements were prepared by incorporating silver oxide as potential antimicrobial agent in a polymethyl metacrylate (PMMA) matrix. In order to improve the biomineralisation and biocompatibility of these cements, electrolytic deposition of collagen was performed in a three-electrode electrochemistry system. ATR FTIR and FT Raman analyses demonstrated that collagen adsorption depends on the silver content in samples. In vitro tests, performed in simulated body fluid (SBF) during three weeks of SBF incubation, revealed the release of Ag^+ by a mechanism involving Ca^{2+} and Na^+ ions exchange. The mineralization process upon incubation was confirmed by the ATR FTIR spectra, which evidenced the phosphate characteristic bands of hydroxyapatite, depending on the silver oxide content in the samples.

(Received November 28, 2010; accepted December 22, 2010)

Keywords: Bone cement; Antimicrobial agent; Collagen coating

1. Introduction

Bone cements are acrylic based resins that were first used for joint arthroplasty surgery in 1958. Their function is to fill the space between the prosthesis and the bone, thereby fixing the prosthesis in the place and acting as an interface between the bone and prosthesis allowing load to be transferred during activity. The bone cements are two component systems. The powder component comprises pre-polymerised polymethyl metacrylate (PMMA), an initiator benzoyl peroxide and a radiopaque component. The monomer, methyl methacrylate (MMA) is the main component of the liquid, but usually an activator is included, along with a small amount of hydroquinone to ensure polymerization of the liquid monomer does not take place during storage. During the polymerization process the dough mixture becomes stiff in a short time (10-15 min), which allows the application in situ and the primary fixation of the joint prosthesis [1, 2].

Orthopedic acrylic cements have to fulfill several medical requirements, such as: low values of maximum cure temperature (to avoid thermal necrosis of the bone tissue, during the setting of the cement), moderate setting time (so that cement does not cure too fast or too slow), high values of compressive strength (allowing the cured cement mantle to withstand the compressive loads involved by normal daily activities) [3]. A new biomaterials generation was born by combining bioactivity, biocompatibility and antibacterial properties of materials, either by antibiotic [4,5] or silver loading [6,7]. The use of antibiotic-loaded bone cement is a well-accepted adjunct in the treatment of infected joint arthroplasty and is gaining further application as a method of prophylaxis. The influence of antibiotic inclusion on cement mechanical properties, specifically fatigue, determines its resistance to crack formation and the long-term in vivo structural integrity of the cement. Several factors influence the choice of antibiotic to add to bone cement. The antibiotic must be able to withstand the exothermic temperature of polymerization, be available as a powder, have a low incidence of allergy, and be able to elute from the cement over an appropriate time period. Several bone cements containing antibiotics such as erythromycin,

colystin, gentamicin and tobramycin have been commercially available in Europe for many years. On the other hand, silver based antimicrobials capture much attention not only because of the non toxicity of the active Ag^+ to human cells [8,] but because of their novelty being a long lasting biocide with high temperature stability and low volatility. The antimicrobial efficacy of these composites depends on their ability to release the silver ions from these composites upon interaction with biological fluids. Hence, silver doped materials are use as an alternative (or complementary) to antibiotic loaded cements, silver being capable of killing over 650 forms of bacteria, viruses [9].

Collagen comprises 90% of the extracellular matrix of bone and it occupies a key role in the interaction of osteoblasts and their environment. It has been previously demonstrated that collagen coating increases the proliferation of osteoblasts into the calcium phosphate ceramics [10].

In the present study, electrolytic deposition of collagen onto silver/PMMA bone cements was performed, operating at physiological conditions. The collagen layer was investigated by ATR FTIR and FT Raman spectroscopy. Different concentration of Ag_2O was incorporated in acrylic bone cement and the released mechanism of Ag^+ ions in Simulated Body Fluid was interpreted taking into account that long-term silver ion release increases with the maximum water absorption on the polymers used as matrix material, because Ag^+ ions are formed from elemental silver particles in the presence of water, only [11,12].

2. Experimental

The investigated materials were prepared using commercial PMMA based cements as starting material (Biomechanica Ind. Brasil), having the following composition: liquid-methylmethacrylate (monomer) 84.4%, butylmethacrylate 13.2%, N:N dimethyl p- toluidine 2.4%, hidroquinone 20 ppm; powder - methylmethacrylate (copolymer) 87.3%, polymethyl metacrylate 2.7 %, barium sulphate 10%. As antimicrobial agent, Ag_2O particles were incorporated with respect to the total powder amount in a concentration ranging from 0.1% to 4 % w/w, resulting a number of six specimens. Electrolytic deposition of collagen type I, soluble, from calf skin (Fluka) was carried out for each specimen in a three-electrode electrochemistry system with a TraceLab 150 potentiometer, equipped with a Trace Master interface board, working in chronoamperometric mode. In preparing the electrolyte, proper amount of $\text{Ca}(\text{NO}_3)_2$ and $\text{NH}_4\text{H}_2\text{PO}_4$ were dissolved in distilled water to obtain 4.5 mM $[\text{Ca}^{2+}]$ and 9 mM $[\text{PO}_4^{3-}]$. Collagen solution was prepared in a concentration of 1 mg/mL of electrolyte and pH was adjusted to 4.8-5.3. Electrolytic deposition of collagen was realised by keeping the working electrode at the potential value of -2V during 1800 seconds. Upon deposition procedure, samples were rinsed with phosphate buffer and dried. The sample surfaces were analyzed by FTIR spectroscopy using a Spectrum BX Perkin Elmer spectrometer, equipped with MIRacle ATR accessory (ZnSe crystal) and by Micro Raman spectroscopy on a Bruker EQUINOX 55 equipment. FTIR spectra were collected in the wavelength range $4000\text{-}400\text{ cm}^{-1}$ at a nominal resolution of 4 cm^{-1} , with a scanning speed of 32 cm^{-1} , a total of 100 scans being accumulated for each spectrum. Micro Raman spectra were collected at 4 cm^{-1} resolution, with 600 scans and laser power between 100-370 mW. Simulated body fluid (SBF) was prepared according to Kokubo protocol [13]. Electrochemical measurements were performed in SBF in static conditions, upon incubation of the materials during three weeks (with and without collagen coating), using a CyberComm 6500 Multimeter (EUTECH Instruments) equipped with Na^+ , Ca^{++} , Ag^+ ion selective electrodes and data aquisition software. The detection limit using this method is 10^{-6} M for Ag^+ ions, and 10^{-5} M for Ca^{++} .

3. Results and discussion

Many common used coating methods such as plasma spray or sol-gel are not always applicable in the case of bone like implant materials. In the present study, electrolytic deposition of collagen by chronoamperometric method [10] was realised by keeping the working electrode at the

potential value -2V during 1800 seconds, the current during electrodeposition being monitored by the potentiostat as shown in Fig.1.

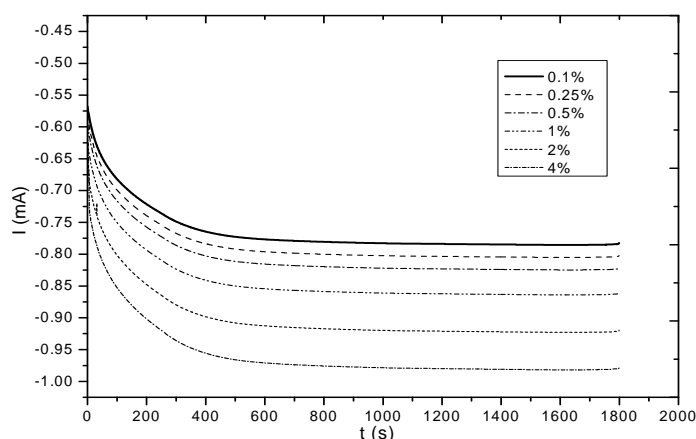


Fig.1. Chronoamperometric curve recorded in collagen-electrolyte solution (1 mg/mL) at -2.0V with respect to the reference cathode, for the specimens with different silver oxide concentration.

The current intensity dropped dramatically in the first few minutes of deposition, then remained relatively constant until ~ 20 min. The rapid decrease in intensity represents the capacitive charging of the electrode, followed by a bearing with approximately constant intensity, limited by the diffusion of collagen concentration [14]. This behaviour is similar for all the samples containing different Ag_2O contents. Visual examination during deposition found that the current drop was associated with the formation of a cloudy and partially transparent gel-like coating on the material surface. This mechanism has been successfully applied to the deposition of calcium phosphates, including hydroxyapatite on conducting substrates [15,16] or calcium phosphate coating containing silver [17]. ATR FTIR and FT Raman spectrometric measurement was carried out to further clarify the presence of collagen coating on the surface of each specimen. The spectra recorded before and after collagen electrodeposition on PMMA-based bone cement are presented comparatively for each specimen in Fig.2. The marker bands of PMMA are a sharp and intense peak at 1722 cm^{-1} due to the presence of ester carbonyl group $\nu(\text{C}=\text{O})$ stretching vibration, a broad band at 1436 cm^{-1} due to $\delta(\text{CH}_3)$ vibration mode, the peaks in the range $1260\text{-}1000\text{ cm}^{-1}$ assigned to O-C-O, C- CH_3 and C-COO stretching vibrations, and the region between $950\text{-}650\text{ cm}^{-1}$ due to the bending of C-H bond [18, 19]. Also in the low wavelength range, some characteristic bands of Ag_2O are present at 640 and 580 cm^{-1} as an asymmetric O-Ag-O bending mode [20]. The PMMA characteristic vibrations are very similar for all the six specimens prepared in this study. The ATR FTIR spectra recorded after electrodeposition confirms the presence of the collagen on the samples surfaces throughout the characteristics of the distinct peaks of collagen: amide I at 1635 cm^{-1} (C=O stretching), amide II at 1550 cm^{-1} (N-H deformation) and amide III around 1200 cm^{-1} (combined N-H bending and C-N stretching).

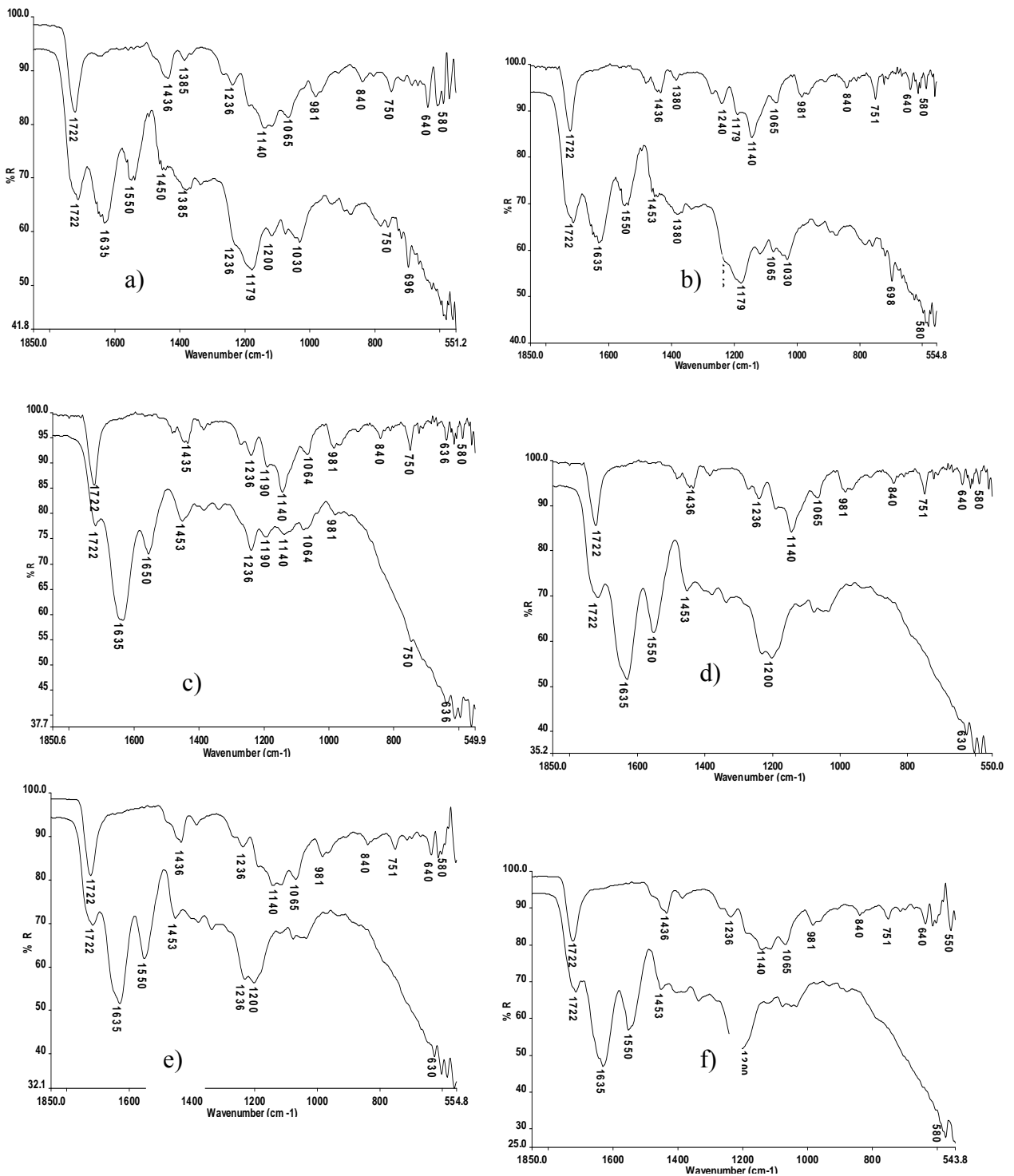


Fig.2 ATR FTIR spectra recorded on the samples surface before (upper spectrum) and after collagen electrodeposition (lower spectrum) with respect to each specimen: a) 0.1%, b) 0.25%, c) 0.50, d) 1% e) 2% and f) 4% silver oxide.

The intensity of these bands is very different with respect to each specimen showing that the maximum deposition of collagen was realized on the samples containing 0.5% and 1% silver, as the amide I band reach the maximum intensity compared with the rest of the samples. More precisely, the relative intensity of collagen amide I band toward the $\nu(\text{C}=\text{O})$ stretching vibration of PMMA vary depending on the quantity of collagen deposited on the surface of each specimen. The

results are in accordance with previous reported study regarding collagen self assembly coating by electrolysis on silicate cathode surface [10].

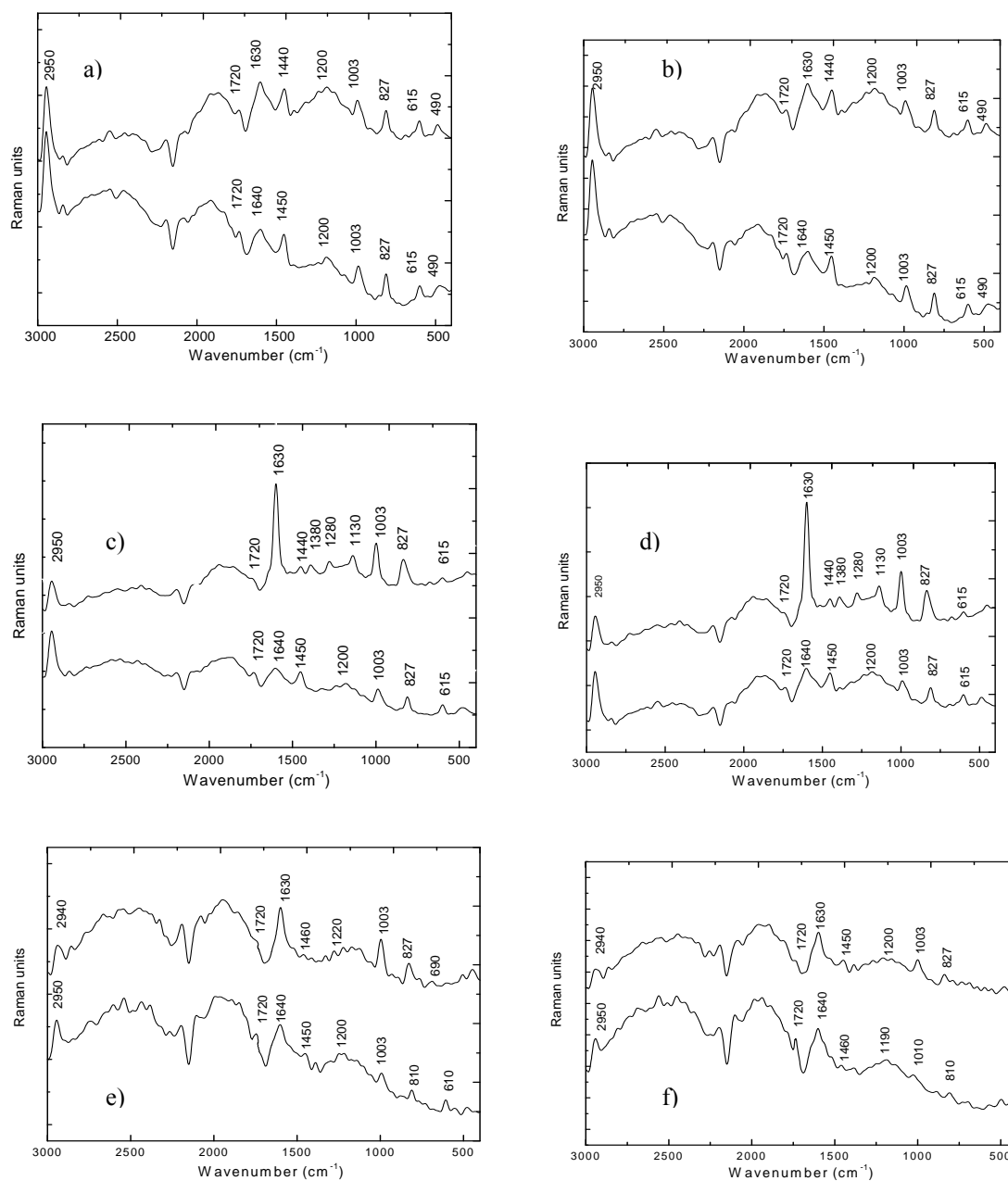


Fig.3. FT Raman spectra recorded on the samples surface before (upper spectrum) and after collagen electrodeposition (lower spectrum) with respect to each specimen: a) 0.1%, b) 0.25%, c) 0.50%, d) 1%, e) 2% and f) 2% silver oxide.

In order to obtain complementary information on the surface modifications upon collagen deposition, FT Raman analysis was applied for each specimen before and after electrodeposition. The recorded spectra are presented comparatively in Fig.3. The main Raman scattering transitions have been observed in PMMA spectra located at 1720 and 1640 cm^{-1} . These transitions are assigned to a stretching mode of the C=O bond in the ester carbonyl group present in both monomer and polymer, and to a stretching mode of the C=C bond present in the monomer only, respectively. According to literature [21,22] the ratio of their intensities should therefore provide a measure of the mass percentage of the uncovered monomer inside the polymer. Other transitions are related to $\delta(\text{CH}_3)$ vibration mode at 1450 cm^{-1} , C-O-C stretch vibration at 1003 cm^{-1} , CH_2

rocking vibration at 827 cm^{-1} , while in the low region the bands 615 and 490 cm^{-1} are the Raman vibrations of Ag_2O . Upon collagen deposition, the relative intensities of the Raman bands are strongly modified and shifted. According to the literature [23] the collagen matrix is related to the Raman bands 1650 cm^{-1} (amide I), 1440 cm^{-1} (amide II), and around 1200 cm^{-1} (amide III). As a general behavior, the band at 1720 cm^{-1} appears weaker and the band at 1640 cm^{-1} is enhanced and low shifted in all the spectra recorded after the electrodeposition procedure. It can be noticed that the strongest enhancement of the band at 1640 cm^{-1} appears for the samples with 0.5 % and 1% silver oxide content along with a low shifted with 10 cm^{-1} upon the collagen adsorption. This behavior indicate a reaction between the collagen layer and PMMA substrate and can be attributed either to hydrogen bonding or to the formation of a new functional group, as the OH deformation band usually appears in the range $1600\text{-}1640\text{ cm}^{-1}$, overlapping the amide I band. If hydrogen bonding occurs, it would involve a weak shift of the carbonyl bond ($\text{C}=\text{O}$), making the observation more difficult with Raman spectroscopy. In the IR spectra, frequencies associated with carbonyls (1720 cm^{-1}) are generally not noticeably shifted by hydrogen bonding. In fact, the carbonyl peak is assigned to both non-bonded and H-bonded carbonyls [23, 24].

The silver ion released in simulated body fluid was monitored during 21 days incubation of the six specimens. The results presented in fig.4 indicate that the silver ion concentration in fluid increase with increasing silver oxide content in the sample. A small amount of silver was detected after the first ten hours of incubation, the Ag^+ release showed only a marginal increase during the first 3 days followed by an abrupt rise after one week especially for composites containing higher silver oxide concentrations.

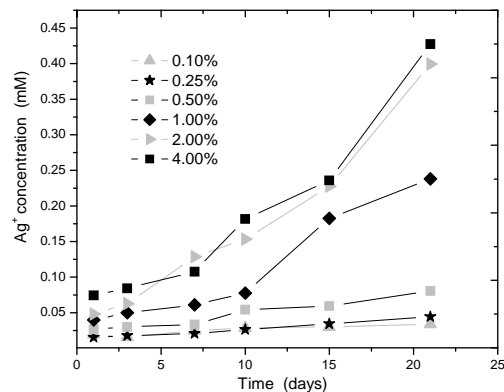


Fig.4. Kinetics of Ag^+ release from the specimens with diferent silver oxide content, during 21 days incubation in SBF.

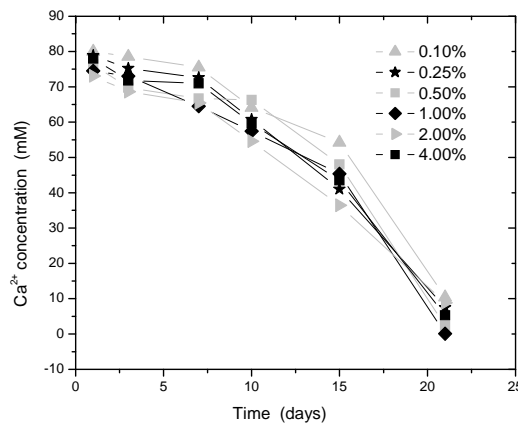


Fig.5. Ca^{2+} concentration in SBF during 21 days incubation of the specimens with diferent silver oxide concentrations.

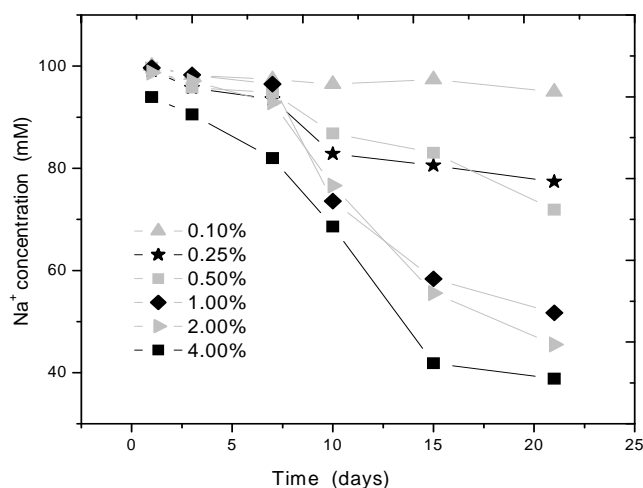


Fig.6. Na⁺ concentration in SBF during 21 days incubation of the specimens with different silver oxide concentrations.

Concomitant, a considerable diminution of Ca²⁺ concentration (two order of magnitude) after 21 days incubation is revealed (Fig. 5) and Na⁺ content decreased one order of magnitude as shown in Fig. 6. The silver release mechanism can be described as follow: in the presence of the sodium or calcium ions characteristic of body fluids, the antimicrobial agent ions exchange with these physiological cations. Long chain hydrophilic polymers incorporated in the coating adsorb water molecules and facilitate the ion exchange [25,26]. In the first few days, the release occurs at the expense of the silver particles confined to the surface layers. This can be instantaneous, because the water molecules need not diffuse well into the specimens. The sudden increase after one week was attributed to plasticization of the specimens after one week of continuous diffusion. So, rather than exhibiting a huge “spike” of activity that diminishes rapidly over time - and that may be toxic to the surrounding tissues - the new biomaterials could prevent bacterial adherence by its slow ion-exchange release of anti-microbial agents. The bioactivity of the surface layer of the specimens was demonstrated by ATR FTIR spectra recorded after 21 days incubation in SBF as shown in Fig. 7. A pronounced decrease in intensity of the bands related to the polymer matrix and to the collagen layer is observed when compared with the corresponding spectra before incubation. Especially for the amide I and II bands of collagen, a broadening and shift to lower wavenumbers was found. The surface mineralization was demonstrated by the strong band at 1020 cm⁻¹ and additionally triplet in the range 630-550 cm⁻¹ which are the characteristic vibrations of the calcium phosphate in hydroxyapatite-type biomimetic coatings [10,27, 28]. The appearance of a new band as a shoulder at 1086 cm⁻¹ is also an indicative of the P-O antisymmetric vibration. Thus, as already reported [28], the cations as well as the anions can be readily and reversibly exchanged. The hydrated collagen layer is not stable and it is progressively replaced by apatite during ageing in an aqueous media (maturation). The mechanism of this transformation is not yet well known but it involves a decrease of the amount of HPO₄²⁻ ions and an increase of the calcium content of the mineral phase. Simultaneously OH⁻ ions are included in the structure and water is excluded [24]. Comparing the spectra in Fig. 7, the sharpness and the intensity of the phosphate bands demonstrate an intense mineralization process on the surface of the specimens containing 0.5, 1.0 and 2% silver oxide.

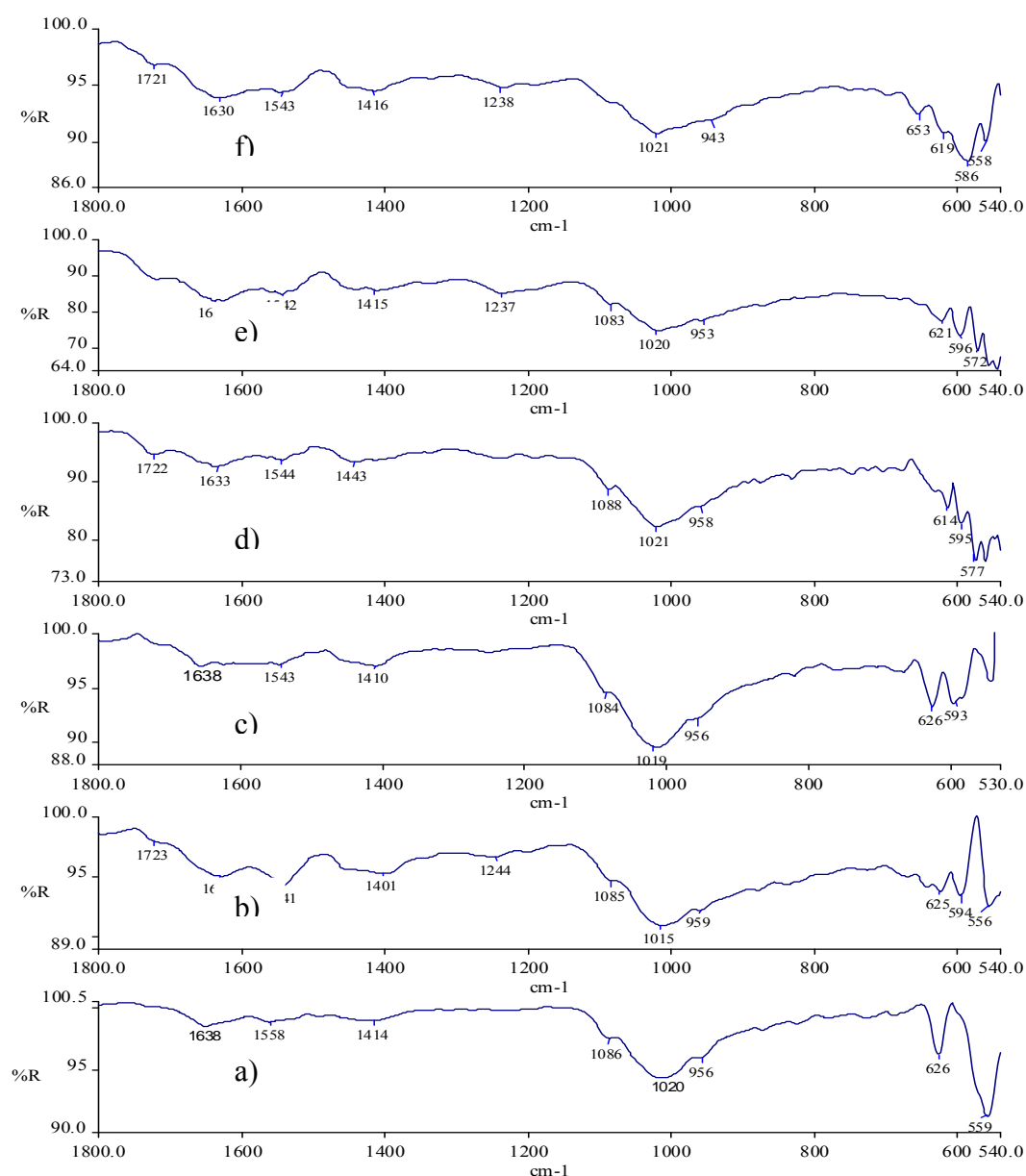


Fig.7. ATR FTIR spectra recorded after 21 days incubation in simulated body fluid of the specimens with different silver oxide content: a) 0.1%, b) 0.25%, c) 0.5%, d) 1%, e) 2 and f) 4% Ag_2O (w/w).

4. Conclusions

Methyl methacrylate based biocomposites are prepared by incorporating different silver oxide content as a potential antimicrobial agent. Collagen electrodeposition on the surface was realised in order to improve the biomineralisation and biocompatibility of the materials. The ATR FTIR and FT Raman results showed that collagen adsorption depends on the silver content in samples. In vitro tests, carried out in simulated body fluid, revealed that the materials are capable to release Ag^+ during three weeks incubation by a mechanism involving Ca^{2+} and Na^+ ions exchange. This mechanism indicated that the Ag^+ ion concentration in fluid increases with increasing Ag_2O content in the sample. The mineralization process was also dependent on the Ag_2O content in the samples.

References

- [1] A.Nizihou, L. Attias, P. Sharrock, A. Ricard, Powder Technol **99**, 60 (1998).
- [2] M. K. D. Nicholas, M. G. J. Waters, K. M. Halford, J Mater Sci: Mater Med **18**, 1407 (2007).
- [3] M. C. Rusu, D. L. Rusu, M. Rusu, JOAM –Symposia **1**(6,) 1020 – 1026(2009)
- [4] Y.He, J.P. Trotignon, B.Loty, A. Tcharkhtchi, J. Verdu, J Biomed Mater Res **63**, 800(2002).
- [5] H.Van de Belt, D.Neut, W. Schenk, J.R.Van Horn, H.C. Van der Mei, H. J. Busscher, Acta Orthop Scand **72**, 557(2001).
- [6] R.Kumar, H.Munstedt, Biomaterials **26**(14), 2081(2004).
- [7] M.Kawashita, S.Tsuneyama, F.Miyaji,T.Kokubo, K.Yamamoto, Biomaterials **21**, 393 (2000).
- [8] J.Hardes, A. Streitburger, H. Ahrens, T. Nusselt, C. Gebert, W. Winkelmann, A.Battmann, G. Gosheger, Sarcoma, doi:10.1155/2007/26539 (2007)
- [9] A. Gupta, S. Silver, Nat Biotechnol **16**, 888(1998)
- [10] Y. Fan, K. Duan, R. Wang, Biomaterials **26**(14) 1623-1632(2005)
- [11] C. Damm, H. Münstedt, Appl Phys A **91** 479-486 (2008).
- [12] S.Cavalu, V.Simon, C. Albon, C. Hozan, JOAM **9**(3) 693-697 (2007)
- [13] T.Kokubo, S.Ito, Z.T.Huang, T.Hayashi, S.Sakka, T.Kitsugi, T.Yamamuro, J Biomed Mater Res **24**, 331(1990).
- [14] C. Cofan, C. Radovan, Sensors **8**, 3952-3969(2008)
- [15] M.C. Kuo, S.K.Yen, Mater Sci & Eng C **20**,153-160 (2002).
- [16] I. Zhitomirsky, Adv Colloid Interface Sci **97**, 279-317 (2002).
- [17] Y. Shibata, H. Yamamoto, T. Miyazaki, J Dent Res **84**(9), 827-831(2005)
- [18] A. Balamurugan, S. Kannan, V. Selvaraj, S. Rajeswari, Trends Biomater Artif Organs **18**(1) 41(2004).
- [19] I. Notinger, J.J. Blaker, V. Maquet, L.L. Hench, A. Boccaccini, Asian J. Physics **15**(2) 221(2006).
- [20] G. I. N. Waterhouse, G. A. Bowmaker,J. B. Metson, Phys Chem Phys **3**, 3838-3845(2001).
- [21] F. Pallikari, G. Chondrokoukis, M. Rebelakis, Y. Kotsalas, Mat Res Innovat **4**, 89-92(2001).
- [22] C. P. Hagan, J. F. Orr, C. A. Mitchell, N.J. Dune, J Mater Sci: Mater Med **20**, 2427-2431(2009).
- [23] J.Xu,I. Stangel, I.S. Butler, D.F.R. Gilson, J Dent Res **76**, 596-601(1997).
- [24] P. Sutandar, D.J.Ahn, E.I.Franses, Macromolecules **27**,7316-7328 (1994).
- [25] C. Damm, Polymers&Polymer Composites **13** (7) 649-656(2005).
- [26] R.Kumar, S. Howdle, H. Münstedt, J Biomed Mater Res Part B:Appl Biomat **75B**, 311–319(2005).
- [27] S. Roessler, R. Born, D. Scharnweber, H. Worch, J Mater Sci Mater Med **12**, 871-877(2001)
- [28] S. Cavalu, V. Simon, J. Optoelectron. Adv. Mater. **8**(4) 1520-1523(2006).